



## Short communication

Effects of radio-frequency sputtering powers on the microstructures and electrochemical properties of LiCoO<sub>2</sub> thin film electrodesHuaijian Pan<sup>a,b</sup>, Yong Yang<sup>a,\*</sup><sup>a</sup> State Key Laboratory for Physical Chemistry of Solid Surfaces, Department of Chemistry, College of Chemistry and Chemical Engineering, Xiamen University, Xiamen, 361005, PR China<sup>b</sup> Department of Chemistry, Binzhou University, Binzhou, 256600, PR China

## ARTICLE INFO

## Article history:

Received 6 August 2008

Received in revised form

12 September 2008

Accepted 15 September 2008

Available online 27 September 2008

## Keywords:

Thin film battery

LiCoO<sub>2</sub> thin film

As-deposited thin film

RF sputtering technique

## ABSTRACT

Different LiCoO<sub>2</sub> thin films are prepared with radio-frequency (RF) sputtering technique. The physical and electrochemical properties of the films are characterized with X-ray diffraction (XRD), Raman scattering spectroscopy (RS), scanning electron microscopy (SEM), energy dispersive spectroscopy (EDS) and charge–discharge experiments. The films obtained at high sputtering power such as 150 W or 200 W which are composed of bigger particles or larger pieces of the target material exhibit better electrochemical performance than the films obtained at low sputtering powers. It should avoid further annealing process of the thin film electrodes. The experimental results have explained why the as-deposited films become better crystallized and therefore their charge–discharge performance is further improved with the increase of the sputtering power.

© 2008 Elsevier B.V. All rights reserved.

## 1. Introduction

The design of high-performance portable electronic devices and electrical equipments requires a large number of very small power sources either in size or weight. In this respect, rechargeable thin film batteries have a great potential in applications to meet this requirement [1–3]. A major reason for this is that they are completely in a solid state and can be fabricated in a variety of shapes, but no gas is generated during operation [4]. In commercial lithium secondary batteries, LiCoO<sub>2</sub> has been widely used as cathode material due to its advantages of high specific capacity, high operating voltage, and long cycle-life [5,6]. LiCoO<sub>2</sub> thin film electrodes have been also fabricated by various thin film deposition techniques including MOCVD [7], spin-coating using sol–gel solutions [8,9], radio-frequency (RF) magnetron sputtering [10–13] and pulsed laser deposition (PLD) [14–18]. However, nearly all of the film electrodes need post-annealing at high temperature [6,19–21] before they are used as cathodes in the thin film batteries. Since those preparation techniques such as RF sputtering technique normally make amorphous LiCoO<sub>2</sub> thin film at low temperatures, a post-annealing process is then required for as-prepared film to form a crystallized LiCoO<sub>2</sub> layer structure. Although the annealing process of the materials can improve the microstructure of the

films, many cracks may be easily formed in the process due to expansion and shrinkage of the films [19]. The high temperature annealing process also has some other disadvantages. For example, it may affect the soldering points of the circuits on the circuit-board, limiting the choice of the flexible and low temperature materials as substrates [22] and can even cause serious interfacial reactions between cathode material and current collecting substrate, degrading the performance of devices to be integrated by thin film batteries [23]. In fact, even flexible batteries are urgently needed today for the flexible and bendable soft portable electronic equipment, such as rollup displays and wearable devices [24]. Thus, it is necessary and important to explore the ways to obtain high-performance as-deposited thin films without the post-annealing process.

In this work, we prepared LiCoO<sub>2</sub> films with RF sputtering technique at different sputtering powers. The physical and electrochemical properties of the as-deposited films were then characterized with different measurements. Based on the experimental results, we have suggested a mechanism that explains reasonably the variations of the physical properties of the as-deposited LiCoO<sub>2</sub> films.

## 2. Experimental

LiCoO<sub>2</sub> films were grown using an RF magnetron sputtering system on Pt wafer substrates from a LiCoO<sub>2</sub> target 78 mm diameter × 5 mm thick, the base pressure was blow  $2.1 \times 10^{-3}$  Pa. The

\* Corresponding author.

E-mail address: [yyang@xmu.edu.cn](mailto:yyang@xmu.edu.cn) (Y. Yang).

distance between the target and the substrates was 55 mm. In order to eliminate impurities on the surface of  $\text{LiCoO}_2$  target, a pre-sputtering treatment was performed for 20 min at 100 W under Ar prior to  $\text{LiCoO}_2$  film growth.  $\text{LiCoO}_2$  films were then deposited at different sputtering powers under a working pressure of 0.5 Pa. The growth temperature (the temperature in the sputtering chamber) was kept below  $55^\circ\text{C}$  and the flow rate ratio of  $\text{Ar}/\text{O}_2$  was 2/1. The as-deposited  $\text{LiCoO}_2$  films were then characterized using a microbalance (METTLER TOLEDO) for film weight, by scanning electron microscopy (SEM, Oxford Instrument LEO 1530) to evaluate thin film thickness, surface grain size and surface morphology, by energy dispersive spectroscopy (EDS, Oxford Instrument) for film composition and by X-ray diffraction (XRD, Philip Panalytical X'Pert) and Raman scattering spectroscopy (RS, BILOR-1 France) for microstructure. To characterize the electrochemical properties of the  $\text{LiCoO}_2$  thin films, CR2025 button cells were fabricated with  $\text{LiCoO}_2$  film and Li foil as cathode and anode, respectively. The electrolyte was 1 M  $\text{LiPF}_6/\text{EC} \pm \text{DMC}$  (1:1) and all the cells were fabricated in an Ar filled glove box (MBRAUN LabMater-100G, Germany). The cells were cycled at room temperature by a home-made discharge and charge equipment (LAND-CT2001A). The cells were initially charged to 4.2 V and then did charge–discharge cycling between 4.2 V and 3 V at a constant current of  $20 \mu\text{A cm}^{-2}$ .

### 3. Results and discussion

#### 3.1. Charge–discharge experiments

Fig. 1 shows a series of discharge curves of the as-deposited  $\text{LiCoO}_2$  films grown at different RF sputtering powers; it also presents a typical discharge curve of the annealed  $\text{LiCoO}_2$  film electrodes for a comparison. It is shown that the discharge capacity of the film obtained at 80 W is about  $54.5 \mu\text{A h cm}^{-2} \mu\text{m}^{-1}$  and its discharge curve is a slope curve without distinctive discharge plateau. With the increase of sputtering power, the discharge capacity of the as-deposited film increases, and the corresponding discharge curve becomes better-shaped. It shows that discharge capacity of the film obtained at 200 W is about  $61 \mu\text{A h cm}^{-2} \mu\text{m}^{-1}$ , which approaches the theoretical capacity ( $64 \mu\text{A h cm}^{-2} \mu\text{m}^{-1}$ ) of  $\text{LiCoO}_2$  thin films, and its discharge curve exhibits a quite well-shaped discharge plateau.

The cycle stability of the as-deposited film and the annealed sample is shown in Fig. 2. For films grown at lower power, the capacity fading is much faster than that of the films at higher power. From the figure, it is obvious that the films obtained at higher pow-

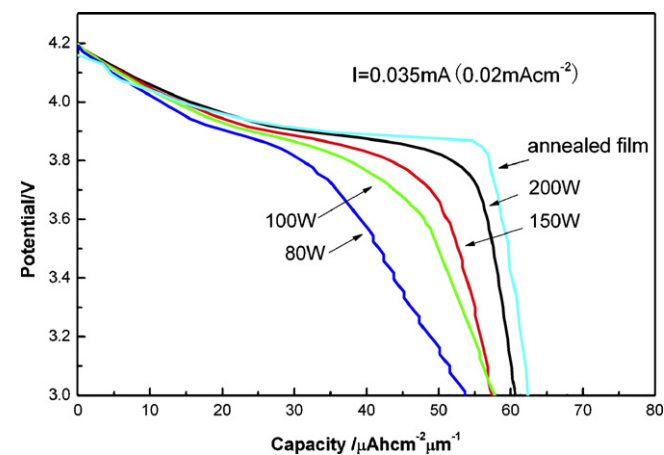


Fig. 1. A comparison of discharge performance of the  $\text{LiCoO}_2$  films grown at different RF sputtering powers and the annealed  $\text{LiCoO}_2$  film.

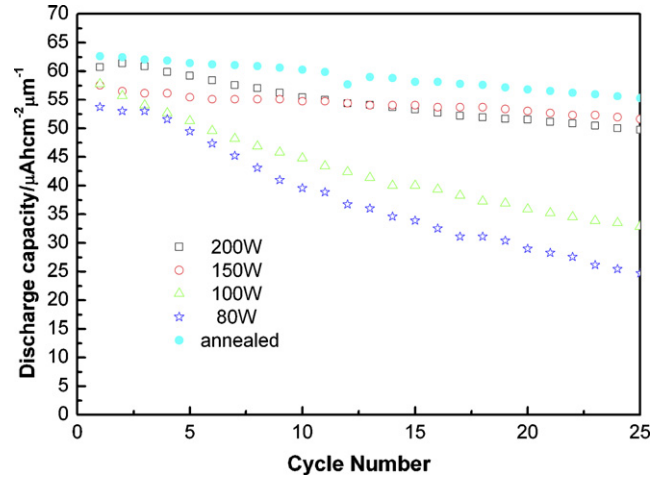


Fig. 2. Cycle stability of the as-deposited  $\text{LiCoO}_2$  films obtained at different RF sputtering powers and the annealed sample.

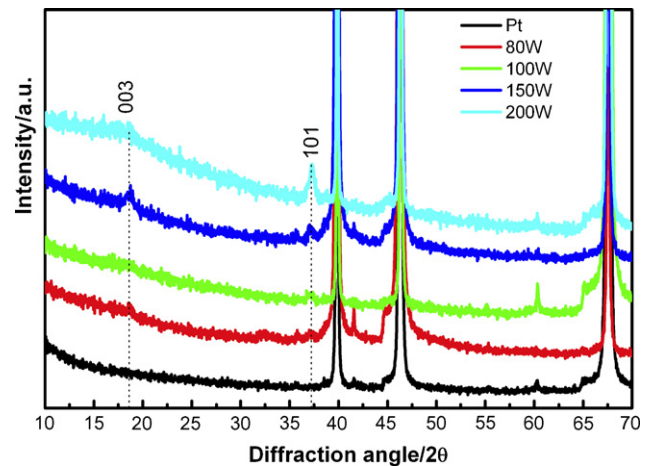
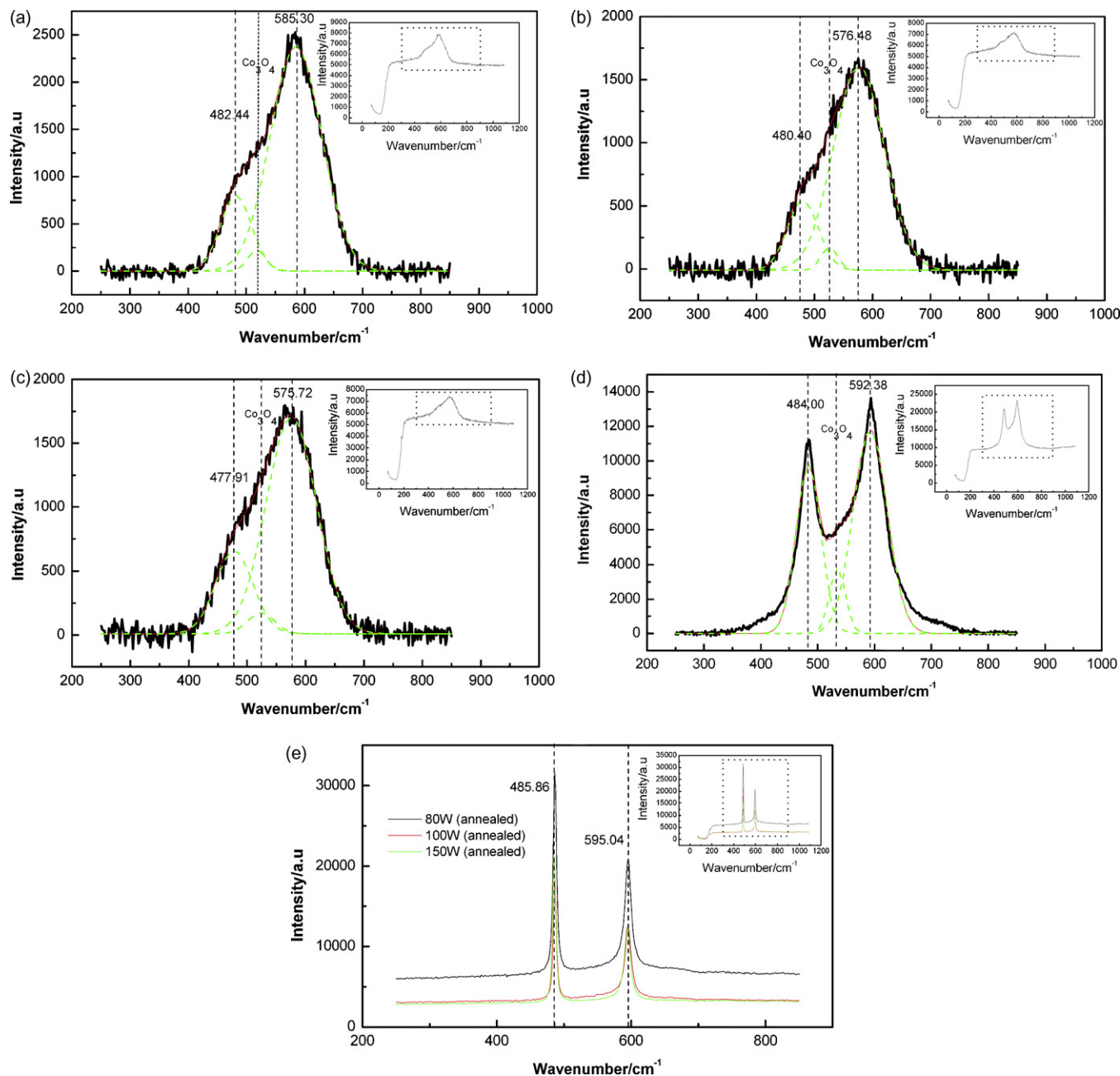


Fig. 3. X-ray diffraction patterns of the films obtained at different RF sputtering powers.

ers of 150 W and 200 W possess quite good capacity retention. After 25 cycles, the capacity retention of the films of 150 W and 200 W are over 88% of their initial discharge capacities, while those of the films at lower powers such as 100 W and 80 W are below 65% of their initial ones, which indicates that increasing sputtering power can also enhance the cycle stability of as-deposited films. Comparing the discharge capacity and the capacity retention of the

Table 1  
EDS data for  $\text{LiCoO}_2$  films grown at different powers.

Power	Element	Weight%	Atomic ratio%
80 W	O K	46.37	76.11
	Co K	53.63	23.89
	Total	100.00	100.00
100 W	O K	44.78	74.92
	Co K	55.22	25.08
	Total	100.00	100.00
150 W	O K	44.07	74.38
	Co K	55.93	25.62
	Total	100.00	100.00
200 W	O K	36.91	68.31
	Co K	63.09	31.69
	Total	100.00	100.00



**Fig. 4.** Raman spectra for as-deposited films grown at different RF sputtering powers of (a) 80 W, (b) 100 W, (c) 150 W and (d) 200 W and (e) for annealed films. The inset is the original RS spectrum for the corresponding film.

as-deposited films grown at higher RF sputtering powers with those of the annealed film, we see that the as-deposited films by high sputtering powers, such as 150 W and 200 W, though their capacities are slightly less than that of the annealed film, have capacities big enough to be practically used in thin film battery instead of the annealed films, therefore avoiding the negative influence of high temperature annealing process [23].

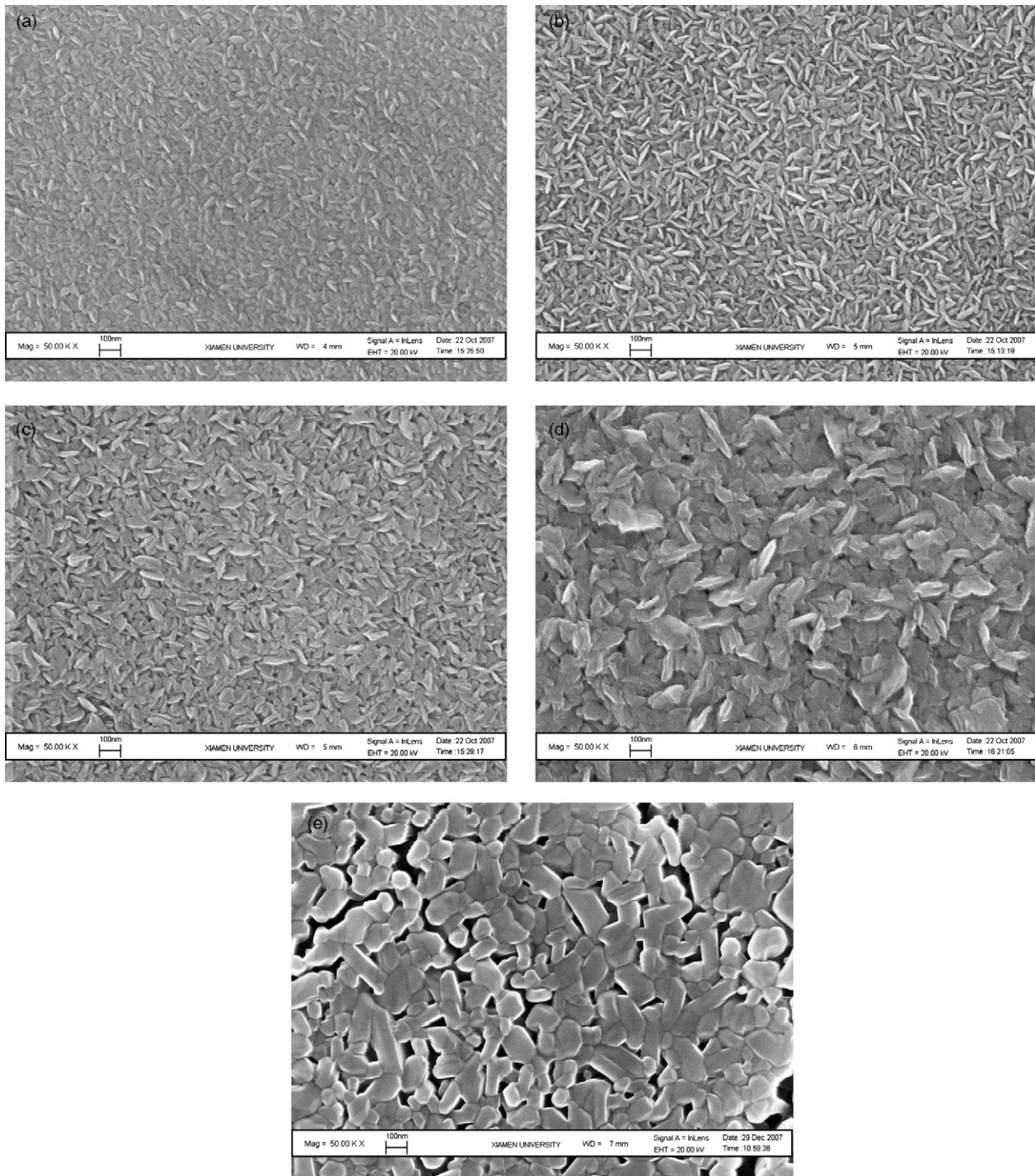
### 3.2. XRD measurement

Fig. 3 shows the X-ray diffraction patterns of the films obtained on Pt substrate at different RF sputtering powers. Due to the Pt substrate, only (003) and (101) diffraction peaks of  $\text{LiCoO}_2$  films can be distinguished. The XRD patterns of as-deposited films of 80 W and 100 W possess very weak diffraction peaks (003) and (101),

while those of 150 W and 200 W possess relatively strong diffraction peaks, the film of 200 W even possesses quite sharp diffraction peak, in particular. From the figure we know that only amorphous or nano-crystalline thin films can be obtained at 80 W and 100 W and that even crystalline thin films can be obtained at 150 W and 200 W. Therefore, it indicates that the crystallized structure of the films is improved with the increase of sputtering power.

### 3.3. Raman spectroscopy measurement

It is well-known that Raman scattering spectrum can reflect the degree of crystallized state of the material. If the material is well crystallized, the Raman scattering peaks are often sharp with strong scattering intensity; while for the amorphous or nano-crystalline material the Raman scattering peaks will broaden and even red



**Fig. 5.** SEM images for the as-deposited  $\text{LiCoO}_2$  films on Pt-substrate obtained at different RF sputtering powers of (a) 80 W, (b) 100 W, (c) 150 W and (d) 200 W and (e) for the annealed sample.

shift with scattering intensity getting weak. Fig. 4 shows Raman scattering spectra for the  $\text{LiCoO}_2$  films obtained under different conditions. Fig. 4(a)–(d) shows RS spectra for the as-deposited films grown at powers of 80 W, 100 W, 150 W and 200 W respectively. Fig. 4(e) shows RS spectra for the annealed films of different powers. The scattering peaks for the films of 80 W, 100 W and 150 W become broad and red-shifted, indicating that all these three films are nano-crystalline which is consistent with the XRD results. It can also be seen from Fig. 4 that the peak positions of as-deposited films of 80 W, 100 W and 150 W corresponding to  $E_g$  and  $A_{1g}$  of the

$\text{LiCoO}_2$  film structure are red-shifting in turn, we think this may be due to the fact that Li/Co ratio in the films increases as the sputtering power increases [23] since larger Li/Co ratio will weaken the strength of the vibrations corresponding to  $E_g$  and  $A_{1g}$ . Such differences apparently come from as-deposited films and the annealed films, the Raman scattering peaks of the as-deposited film of 200 W at the positions of  $484\text{ cm}^{-1}$  and  $592\text{ cm}^{-1}$  are quite sharp and their positions have very small red shifts, which means that the 200 W as-deposited film is quite well crystallized. It is of significance to indicate here that Raman scattering peaks of the annealed films

deposited at different powers have almost the same positions of  $486\text{ cm}^{-1}$  and  $595\text{ cm}^{-1}$  which correspond to RS peaks  $E_g$  and  $A_{1g}$ , respectively. In addition, we can see from Fig. 4 that in all the as-deposited films  $\text{Co}_3\text{O}_4$  phase exists, while in the annealed films no  $\text{Co}_3\text{O}_4$  phase has been found.

### 3.4. SEM images and EDS data

Fig. 5 presents SEM images of the top-surfaces of as-deposited  $\text{LiCoO}_2$  films obtained on Pt substrate at different RF sputtering powers and the annealed sample. The surface morphologies of the as-deposited films at different sputtering powers are all smooth and crack-free. The films are stacked with small slender particles or irregular flat thin pieces of the parent material. The images show clearly that the sizes of the particles which form the films become much bigger with the increase of the sputtering power. Statistically, the particle sizes are about 40 nm, 80 nm, 100 nm, and 150 nm for the as-deposited films at different sputtering powers of 80 W, 100 W, 150 W, and 200 W, respectively.

Table 1 presents some data of EDS for  $\text{LiCoO}_2$  films obtained at different sputtering powers. From the table, we can see that the atomic ratio of Co/O for the films is approaching the ratio for the target material  $\text{LiCoO}_2$  as the sputtering power increases. Though the data of EDS cannot be used as the accurate measurement of compositions of the films, at least, they show us clearly a tendency in the changes in the composition of the films.

### 3.5. Discussion

Now we put all the experimental results together for consideration. Generally, as-deposited  $\text{LiCoO}_2$  films are thought to be amorphous or nano-crystalline. According to our work, the amorphous films are grown at lower sputtering powers, while the nano-crystalline or even well-crystalline films are grown at higher powers. Greater powers improve the layer structure of the as-deposited films, so further improve the electrochemical properties of the films. We think that the reason why increasing sputtering powers can improve the microstructure of the as-deposited films is that the changes of sputtering power result in the changes of the sputtering mechanism. As sputtering power increases, the forces of the bombardment on the target by plasma will increase, bigger particles of the target material may be directly deposited on the substrates. If the powers are great enough, even big pieces of the target material may be flaked-off. From SEM images of the top-surfaces of the films, it is clear that the sizes of the particles constituting the films get bigger as the sputtering power increases. At power of 200 W, the films are composed of irregular flat thin pieces of the target material, the pieces being sharp-edged and different apparently from surface features of the annealed film which, we can see from Fig. 5(e), is usually composed of smooth-edged particles. If the sputtered or flaked-off particles are relatively big, the films will remain properties of the target material to some extent, for instance, the crystallinity and the composition of the target material. The rationality of this suggested mechanism is supported by the facts that as the sputtering power increases, the degree of crystallization of the films become better and better and the compositions of the films further approach the composition of the target material. And we can also explain why  $\text{Co}_3\text{O}_4$  exists apparently in the films obtained at low sputtering power of 50 W, but exists in very small amount

in the films obtained at high powers [23]. At low powers, the sizes of the particles sputtered off the target are small, even as small as atomic sizes,  $\text{Li}^+$  ions can be easily lost during sputtering process; at high powers, the particles are so big that the loss of  $\text{Li}^+$  ions may only occur on the surface of the particles, greatly reducing the loss of  $\text{Li}^+$  ions in the films.

## 4. Conclusions

By controlling the sputtering powers, we have obtained as-deposited  $\text{LiCoO}_2$  films with different physical and electrochemical properties. Controlling the sputtering powers during RF magnetron experiments means to control the sizes of the particles sputtered from the target material. The particle size of the active material determines the properties of the as-deposited films. If the sputtering powers are big enough, the as-deposited  $\text{LiCoO}_2$  films will be composed of big particles or large flat thin pieces of target material, which will remain the properties of the target material to some extent. The  $\text{LiCoO}_2$  films obtained at high powers of 150 W and 200 W could practically be used as thin film cathodes in thin film batteries instead of the annealed  $\text{LiCoO}_2$  thin films, avoiding the negative effects of the high temperature annealing process.

## Acknowledgment

We are grateful that this work is supported by the National Basic Research Program of China (973 Program) (Grant no. 2007CB209702), and National Natural Science Foundation of China (NNSFC, Grant no. 90606015).

## References

- [1] J.B. Bates, G.R. Gruzalski, N.J. Dudney, C.F. Luck, X. Yu, *Solid State Ionics* 70/71 (1994) 619.
- [2] P. Birke, W.F. Chu, W. Weppner, *Solid State Ionics* 93 (1997) 1.
- [3] T. Brousse, P. Fragnaud, R. Marchand, D.M. Schleich, O. Bohnke, K. West, *J. Power Sources* 68 (1997) 412.
- [4] W.S. Kim, *J. Power Sources* 134 (2004) 103–109.
- [5] P. Fragnaud, T. Brousse, D.M. Schleich, *J. Power Sources* 63 (1996) 187.
- [6] B. Wang, J.B. Bates, F.X. Hart, B.C. Sales, R.A. Zuhr, J.D. Robertson, *J. Electrochem. Soc.* 143 (1996) 3203.
- [7] S.I. Cho, S.G. Yoon, *J. Electrochem. Soc.* 149 (2002) A1584.
- [8] Y.H. Rho, K. Kanamura, *J. Electrochem. Soc.* 151 (2004) A1406.
- [9] K.W. Kim, S.I. Woo, K.H. Choi, K.S. Han, Y.J. Park, *Solid State Ionics* 159 (2003) 25.
- [10] C.N. Polo da Fonseca, J. Davalos, M. Kleinlke, M.C.A. Fantini, A. Gorenstein, *J. Power Sources* 81–82 (1999) 575.
- [11] C.L. Liao, K.Z. Fung, *J. Power Sources* 128 (2004) 263.
- [12] W.S. Kim, *J. Power Sources* 134 (2004) 103.
- [13] J.B. Bates, N.J. Dudney, B.J. Neudecker, F.X. Hart, H.P. Jun, S.A. Hackney, *J. Electrochem. Soc.* 147 (2000) 59.
- [14] K.A. Striebel, C.Z. Deng, S.J. Wen, E.J. Cairns, *J. Electrochem. Soc.* 143 (1996) 1821.
- [15] J.D. Perkins, C.S. Bahn, P.A. Parilla, J.M. McGraw, M.L. Fu, M. Duncan, H. Yu, D.S. Ginley, *J. Power Sources* 81–82 (1999) 675.
- [16] J.D. Perkins, C.S. Bahn, J.M. McGraw, P.A. Parilla, D.S. Ginley, *J. Electrochem. Soc.* 148 (2001) A1302.
- [17] C. Julien, S. Gastro-Garcia, *J. Power Sources* 97–98 (2001) 290.
- [18] S.B. Tang, L. Lu, M.O. Lai, *Philos. Mag.* 85 (2005) 2831.
- [19] J.K. Lee, S.J. Lee, H.K. Baik, H.Y. Lee, S.W. Jang, S.M. Lee, *Electrochem. Solid-State Lett.* 2 (1999) 512.
- [20] F.K. Shokoohi, J.M. Tarascon, B. Wilkens, *J. Appl. Phys. Lett.* 59 (1991) 1260.
- [21] N.J. Dudney, *J. Power Sources* 89 (2000) 176.
- [22] J.F. Whitacre, W.C. West, E. Brandon, B.V. Ratnakumar, *J. Electrochem. Soc.* 148 (2001) A1078.
- [23] S.W. Jeon, J.K. Lim, S.H. Lim, S.M. Lee, *Electrochim. Acta* 51 (2005) 268–273.
- [24] H. Nishide, K. Oyaizu, *Science* 319 (2008) 737–738.